Amino Acids (2010) 39:671–683
DOI 10.1007/s00726-010-0488-4

ORIGINAL ARTICLE

Laccase-catalyzed cross-linking of amino acids and peptides with dihydroxylated aromatic compounds

Annett Mikolasch · Veronika Hahn · Katrin Manda · Judith Pump · Nicole Illas · Dirk Gördes · Michael Lalk · Manuela Gesell Salazar · Elke Hammer · Wolf-Dieter Jülich · Stephan Rawer · Kerstin Thurow · Ulrike Lindequist · Frieder Schauer

Received: 16 October 2009 / Accepted: 16 January 2010 / Published online: 9 February 2010

Abstract In order to design potential biomaterials, we investigated the laccase-catalyzed cross-linking between L-lysine or lysine-containing peptides and dihydroxylated aromatics. L-Lysine is one of the major components of naturally occurring mussel adhesive proteins (MAPs). Dihydroxylated aromatics are structurally related to 3,4-dihydroxyphenyl-L-alanine, another main component of MAPs. Mass spectrometry and nuclear magnetic resonance analyses show that the ε-amino group of L-lysine is able to cross-link dihydroxylated aromatics. Additional oligomer and polymer cross-linked products were obtained from di- and oligopeptides containing L-lysine. Potential applications in medicine or industry for biomaterials synthesised via the three component system consisting of the oligopeptide $[Tyr\text{-}Lys]_{10}$, dihydroxylated aromatics and laccase are discussed.

Keywords Laccase · Mussel adhesive proteins · Cross-link · Biomaterial · ε-Amino group

A. Mikolasch (✉) · V. Hahn · J. Pump · N. Illas · F. Schauer
Institute of Microbiology, Ernst-Moritz-Arndt-University Greifswald, Friedrich-Ludwig-Jahn Straße 15, 17487 Greifswald, Germany
e-mail: annett.mikolasch@uni-greifswald.de

K. Manda
Department of Radiotherapy, University Rostock, Südring 75, 18059 Rostock, Germany

D. Gördes
Institute of Automation, University Rostock, R.-Wagner-Str. 31, 18119 Rostock, Germany

M. Lalk · W.-D. Jülich · U. Lindequist
Institute of Pharmacy, Ernst-Moritz-Arndt-University Greifswald, Friedrich-Ludwig-Jahn Straße 17, 17487 Greifswald, Germany

M. Gesell Salazar · E. Hammer
Interfaculty Institute for Genetics and Functional Genomics, Ernst-Moritz-Arndt-University Greifswald, Friedrich-Ludwig-Jahn Straße 17, 17487 Greifswald, Germany

S. Rawer
Applied Biosystems, a part of Life Technologies, Frankfurter Straße 129 B, 64293 Darmstadt, Germany

K. Thurow
Center for Life Science Automation, F.-Barnewitz-Str. 8, 18119 Rostock, Germany

Introduction

Mussel adhesive proteins (MAPs) are remarkable materials which have the ability to lock mussels onto hard, wet surfaces. The structure of mussel adhesive proteins from a number of different marine mussel species have been investigated over the course of the last decades (Waite et al. 1985, 1989; Rzepecki et al. 1991; Vreeland et al. 1998; Zhao and Waite 2006; Zhao et al. 2006; Harrington and Waite 2007; Holten-Andersen et al. 2009b). One common feature of many of the MAPs studied is the high level of the amino acid 3,4-dihydroxy-L-phenylalanine (DOPA). The DOPA residues are thought to play a key role in the chemisorption of the polymers to substrates underwater and to the formation of covalent cross-links within the adhesive (Waite 1990a; Burzio et al. 1997).

However, the abundance of potential reactions of DOPA and *ortho*-quinones (oxidation products of DOPA) creates considerable uncertainty as to the ways in

which different marine mussel species carry out the curing process and all of the mechanisms described to date are largely hypothetical (Waite 1990b; Vreeland et al. 1998).

For this reason, synthetic DOPA-containing polypeptides have been used to experimentally identify the functions and reactions of the amino acids which are active in the chemistry of the MAPs. Synthetic DOPA-containing polypeptides with L-lysine and L-glutamic acid were first used by Yamamoto and Hayakawa (1979, 1982) to show that the adhesion and cross-linking capabilities of mussel adhesive proteins can be successfully reproduced using synthetic materials. In these studies, however, the mechanism of bonding was left unclear.

Many applications have been proposed for synthetic MAPs (Waite 2008) including adhesives for medical (Strausberg and Link 1990), surgical (Green 1995), ophthalmic (Robin et al. 1988), and dental (Holten-Andersen and Waite 2008) applications, as well as for enzyme, cell, and tissue immobilizing agents, anti-corrosives, and metal scavengers (Deming 1999).

Our efforts in this area are focused on the design of a potential biomaterial for biomedical or industrial applications and on the description of the intermolecular bonding mechanisms involved in its formation.

We describe here the design of a potential biomaterial based on (a) MAPs and on (b) the laccase-catalyzed amination of dihydroxylated aromatic compounds (laccase substrates) by amino acids and lysine-containing peptides. Different dihydroxylated laccase substrates (structurally related to DOPA) can be oxidized by the polyphenoloxidase laccase and subsequently aminated by the amino groups of the amino acids tryptophan and phenylalanine to form covalent C–N-bonds (Manda et al. 2006; Hahn et al. 2009a, b). Depending on the substitution degree both monoaminated (one amino acid couples) and diaminated (two amino acids couple) products were formed. These results suggest that both the α- and the ε-amino group of the amino acid lysine, one important component of the MAPs, may be able to participate in the laccase-catalyzed C–N-coupling and subsequent cross-linking. Hence, these enzymatic reactions may be suitable also to cross-link proteins containing large amounts of lysine in the presence of dihydroxylated aromatics. To design potential biomaterials, we focused on three areas: first, to analyze the reaction of lysine with dihydroxylated aromatic compounds; second, to analyze the reaction products of laccase-catalyzed reactions of dipeptides consisting of tyrosine and lysine with dihydroxylated aromatics, and third, to synthesize and analyze cross-linked products of synthetic tyrosine-lysine-containing decapeptides with dihydroxylated aromatics.

Materials and methods

Chemicals

The laccase substrates were purchased from Sigma-Aldrich (2,5-dihydroxybenzoic acid methyl ester, *para*-hydroquinone), from Fluka (hydrocaffeic acid), and from Midori Kagaku Co., Japan (2,5-dihydroxy-*N*-(2-hydroxyethyl)-benzamide). The amino acids and peptides were obtained from Bachem (lysine(Ac)-OH, Ac-lysine-OH, H-Tyr-Lys-OH, Z-[Tyr-Lys]-OH), from Merck (L-lysine monohydrochloride), and from Sigma-Aldrich (L-tyrosine). All chemicals were used as received.

Peptide synthesis

The oligopeptide with the structure $[Tyr\text{-}Lys]_{10}$ was synthesized on an ABI 433A peptide synthesizer (Applied Biosystems, Foster City, CA, USA) using Fmoc-chemistry with UV-monitoring. For coupling, amino acid derivatives were activated by HBTU and the Fmoc-group was released with 20% piperidine in NMP. The following solvents and reagents were used: HBTU activator, Fmoc-Lys(Boc)-OH, Fmoc-Tyr(tBu)-OH, and a preloaded Fmoc-Lys(Boc)-HMP-resin were obtained from Applied Biosystems, except piperidine (Sigma-Aldrich). After assembly, the peptide was cleaved from the resin using a mixture of triisopropylsilane/H_2O/triisopropylsilane (2.5%/2.5%/95%) for 2 h at room temperature. The resin was removed by filtration and the solution was added dropwise to cold methyl *tert*-butyl ether (MTBE) in order to precipitate the peptide. After 5 min centrifugation at 3,000 rpm, the peptide pellet was resuspended in MTBE and the process repeated three times. The final pellet was dried in air and the sample was analyzed by MALDI-MS on a Voyager-DE mass analyzer (Applied Biosystems).

Enzymes

Fungal strain

Pycnoporus cinnabarinus SBUG-M 1044 was isolated from an oak tree in northern Germany. This white rot fungus is deposited in the strain collection of the Department of Biology of the University Greifswald (SBUG).

Cultivation of Pycnoporus cinnabarinus SBUG-M 1044

P. cinnabarinus was initially cultivated on malt agar plates that were incubated for 7 days at 30°C and then kept at 4°C. The liquid culture was prepared by inoculating a nitrogen-rich medium containing 5 g glucose, 1 g KH_2PO_4,

0.52 g L-asparagine, 0.5 g yeast extract, 0.5 g KCl, 0.5 g $MgSO_4 \cdot 7\ H_2O$, 50 mL mineral salt solution and 50 mL $FeSO_4$ solution (0.2 g L^{-1}) with three 1 cm^2 agar culture fragments. The mineral salt solution, modified according to Braun-Lüllemann et al. (1997), contained 1 g $Ca(NO_3)_2 \cdot 4H_2O$, 0.06 g $CuSO_4 \cdot 5H_2O$, and 0.04 g $ZnSO_4 \cdot 7H_2O$ per liter. Incubation was performed without shaking at 30°C for 7 days. A uniform inoculum was obtained by homogenization of this culture with an Ultra-Turrax homogenizer T25 (IKA Labortechnik, Staufen, Germany) at 8,000 rpm. For the production of the ligninolytic enzyme laccase, 40 mL medium inoculated with 2 mL of the homogenized pre-culture was incubated in 100 mL Erlenmeyer flasks for 7 days with 3,4-dimethoxybenzyl alcohol (10 mM), a known inducer of laccase. Cultures were shaken in a water bath (GFL model 1092, Burgwedel, Germany) at 30°C and 158 rpm.

Preparation of laccase from Pycnoporus cinnabarinus SBUG-M 1044 (PcL)

Under these culture conditions, *P. cinnabarinus* produced laccase as an extracellular enzyme with an activity of 500 nmol mL^{-1} min^{-1}. The culture medium was filtered through a glass fibre filter on a Büchner funnel to separate the medium from whole cells. The cell-free culture medium was stirred with DEAE-Sephacel (Sigma, Steinheim, Germany) for 1 h and the adsorbed enzymes were eluted from the DEAE-Sephacel with 20 mM sodium acetate buffer (pH 5). The enzyme extract was desalted using a Sephadex G-25 Superfine column (Pharmacia, Freiburg, Germany). This enzyme preparation contains only isoenzymes of laccase, but no other enzymes and was used in 20 mM sodium acetate buffer (SAB) pH 5.0 which is close to its pH optimum (Eggert et al. 1996; Feng et al. 1996; Jonas et al. 1998).

Laccase from *Myceliophthora thermophila* (MtL, expressed in genetically modified *Aspergillus* sp.) was obtained from Novozymes (Bagsvaerd, Denmark) and used as received (activity 1,000 U/g; substrate: syringaldazine) in citrate phosphate buffer (CPB, 18 mM citrate, 165 mM phosphate) at its pH optimum of pH 7.0 (Feng et al. 1996; Berka et al. 1997).

Measurement of laccase activity

The activity of laccase was determined spectrophotometrically at 420 nm with ABTS (2,2′-azino-*bis*(3-ethylbenzothiazoline-6-sulfonic acid) diammonium salt) as substrate (Bourbonnais and Paice 1990) using the method described by Jonas et al. (1998). 1 U is defined as 1 μmol mL^{-1} min^{-1}.

Experimental procedures

For analytical experiments the respective dihydroxylated compound (1 mM) and the reactants L-lysine, L-tyrosine, Ac-Lys-OH, Lys(Ac)-OH, H-Tyr-Lys-OH, or Z-[Tyr-Lys]-OH (1 mM, 2 mM or 10 mM) were incubated with laccase (activity 0.5 U). Experiments with laccase from *Myceliophthora thermophila* were performed in citrate phosphate buffer (CPB, 18 mM citrate, 165 mM phosphate) at its pH optimum of pH 7.0. Experiments with laccase from *Pycnoporus cinnabarinus* were performed in 20 mM sodium acetate buffer (SAB) pH 5.0. In controls, the respective compounds were incubated in SAB or CPB without laccase. 2 mL of each analytical experiment were incubated with agitation at 200 rpm in 5-mL-brown-glass-bottles at room temperature.

Analytical HPLC

For routine analyses, the reaction mixtures were analyzed using an HPLC system Agilent Technologies, 1200 Series (Waldbronn) consisting of a G1311A quaternary pump, G1322A degaser, G1329A auto sampler, G1315D diode array detector, and Agilent ChemStation. The separation of the substances was achieved on an endcapped, 5 μm, LiChroCART® 125-4 RP18 column (VWR, Darmstadt, Germany) at a flow rate of 1 mL min^{-1}. The solvent gradient consisted of a mix of methanol (eluent A) and 0.1% phosphoric acid (eluent B), starting from an initial ratio of 10% A and 90% B and reaching 100% methanol within 14 min.

Isolation of transformation products

The experimental procedure above was upscaled tenfold for isolation of products for MS and NMR analyses. RP18 silicagel columns (60 mL, 10 g adsorbent material, phenomenex, Strata, Germany) were charged with 20 mL of reaction mixture after product formation. An excess of amino acid or peptide was eluted with buffer (CPB after reaction with MtL and SAB after reaction with PcL) and methanol water mixtures. The cross-coupling products were eluted with 100% methanol. The isolated products were dried by lyophilization prior to mass spectrometry (MS) and nuclear magnetic resonance (NMR) spectroscopy.

Reactions of oligopeptides

For the isolation of oligomer products for MS analysis, 16 mL CPB with MtL and 1 mM hydrocaffeic acid or 2,5-dihydroxy-*N*-(2-hydroxyethyl)-benzamide and 1 mM $[Tyr\text{-}Lys]_{10}$ were used. After an incubation period of 24 h the

mixtures were brown colored and brown precipitates were recovered. The reaction mixtures were centrifuged (10 min, 16,060×*g*) and the supernatants were discarded. The pellets were resuspended in distilled water and dried by lyophilization.

Characterization of the products

The products **3a**, **3c**, **3d**, **3e**, **3f**, **3g$_1$**, **3g$_2$**, **3i**, **4a**, **4d$_1$**–**4d$_4$**, **4f$_1$**, and **4f$_2$** were characterized by liquid chromatography/mass spectrometry (LC/MS). The standard atmospheric pressure ionization (API) mass spectrometry experiments were performed using an Agilent Series 1100 HPLC system and an Agilent 1946C quadrupole mass spectrometer (Waldbronn, Germany). The MS was used with both atmospheric pressure chemical ionization (APCI) and electrospray ionization (API-ES) sources. HPLC separation was performed on a LiChroCART® 125-4, LiChrosphere® 100 RP-18e column (Merck, Darmstadt, Germany) at 25°C at a flow rate of 1 mL min^{-1} within a 14-min gradient from 10 to 100% methanol in 0.1% aqueous formic acid. APCI/API-ES MS conditions (positive and negative ion mode) were as follows: nebulizer and drying gas, nitrogen; nebulizer pressure, 30 psig; drying gas flow, 10 L min^{-1}; vaporizer temperature (for APCI), 350°C; drying gas temperature, 250°C; capillary voltage, 4 kV; corona current (for APCI), 4 µA. LC high-resolution mass spectrometry experiments were performed on an Agilent Series 1200 HPLC system and an Agilent 1969A time-of-flight mass spectrometer (Waldbronn, Germany). The TOF–MS conditions (negative and positive ion mode) with a dual sprayer API-ES source were as follows: nebulizer and drying gas, nitrogen; nebulizer pressure, 40 psig; drying gas flow, 10 L min^{-1}; drying gas temperature, 350°C; capillary voltage, 4 kV; fragmentor voltage, 175 V; skimmer voltage, 60 V; octopole voltage, 250 V; mass reference (*m/z*), 121.05087 and 922.00979 in positive ion mode, and 112.98558 and 1,033.98810 in negative ion mode. HPLC separation was performed on a Zorbax Eclipse XDB-C8, 4.6 mm × 50 mm, 3.5 μ, column (Agilent, Germany) at 25°C at a flow rate of 0.5 mL min^{-1} within a 14-min gradient from 10 to 100% methanol in 0.1% aqueous formic acid.

All FT-ICR MS high-resolution mass spectrometry (HRMS) experiments were performed on a Bruker Daltonics APEX III FT-ICR mass spectrometer (Bremen, Germany) equipped with a 7.0 T shielded superconducting magnet. The flow rate for the eluent (H_2O/ACN/HCOOH 49/49/2, all HPLC-grade) was 2 µL/min using a syringe pump (Cole-Palmer 74900 series). The ions were generated from an external ESI source (Apollo ESI-Source) with the nebulizing gas pressure at 20 psi, heated drying gas at 20 psi and 150°C, and a capillary entrance voltage of −4,500 V in negative ion mode and +4,500 V in positive ion mode (Marshall and Schweikhard 1992; Amster 1996; Marshall et al. 1998).

Mass spectra were acquired with both positive and negative ion modes with broadband detection (32 scans each experiment) from 100 to 2,000 Da using 1,024 K data points. All experimental sequences, including scan accumulation and data processing, were performed with XMASS 6.1.2 on Windows 2000.

The products **3h**, **3i**, **4b$_1$**–**4b$_3$**, **4c**, **4e$_2$**, **4e$_3$**, **4f$_1$**, and **4f$_2$** were analyzed by LC/MS as described previously (Donat et al. 2009). A C-18 column (Merck LichroSpher, 150 mm × 4.6 mm, 5 µm) was used with solvent A: 0.1% formic acid in water and solvent B: acetonitrile. The gradient $t = 0$ min, 10% B; $t = 6$ min, 30% B; $t = 11$ min, 30% B; $t = 17$ min, 70% B; $t = 20$ min, 100% B was used at flow rate 0.5 ml/min. The mass spectrometric parameters were adjusted for positive mode detection as described before (Donat et al. 2009). Reference masses were used from the Agilent "ESI tune mix" as described above.

Digestion of the polymer mixture **5a** of $[Tyr\text{-}Lys]_{10}$ and hydrocaffeic acid **2d** was performed for 3 h at 37°C using Lys C (Sigma) dissolved in 20 mM NH_4HCO_3 (pH 8.2) at a ratio 1:100 (v/v). To purify peptides prior to LC–MS analyses a Zip-Tip method was used (Millipore Corporation). After equilibration of the C_{18} material and binding of the peptide extracts, five wash steps were performed with 10 µL 1% acetic acid to remove contaminations. Peptides were eluted using 5 µl of 50% and subsequently 80% v/v acetonitril, 0.1% v/v acetic acid. The combined eluates were concentrated in a vacuum centrifuge and redissolved in 10 µl of 2% v/v acetonitril, 0.1% acetic acid.

Samples were separated prior to mass spectrometric analyses by reverse phase nano HPLC on a 15 cm PepMap100-column (3 µl, 100 Å) using a Proxeon System (Odense, Denmark) at a flow rate of 1 µl/min. Separation was achieved using a linear gradient from 0.05% acetic acid, 2% acetonitrile in water (A) to 0.05% acetic acid in 45% acetonitrile (B) as eluents for 35 min MS-data were generated using the Orbitrap-MS equipped with a nano-electrospray ion source (PicoTip Emitter FS360-20-20-CE-20-C12, New Objective). After a first survey scan ($r = 60{,}000$) MS^2 data were recorded for the five highest mass peaks in the linear ion trap at a collision induced energy of 35%. The exclusion time was set to 30 s and the minimal signal for MS^2 was 1,000.

The nuclear magnetic resonance (NMR) spectra for the products (^{1}H NMR, ^{13}C NMR, HSQC, HMBC) were recorded on a Bruker Avance 600 instrument (Karlsruhe, Germany) at 600 MHz.

Dimer **3a**. Synthesis (1:1 mM, PcL) and isolation as described above. R_f (HPLC) 8.8 min, UV–Vis (MeOH) λ_{max} 218, 273, 481 nm. MS (LC/MS): *m/z*: AP-ES, pos. ion

mode 346 $[M + H]^+$, 368 $[M + Na]^+$; HRMS FT-ICR ($C_{17}H_{15}NO_7$) calcd: [M] 345.08485; found: $[M + H]^+$ *m/z* 346.09279 (1.94 ppm), $[M + Na]^+$ *m/z* 368.07493 (2.34 ppm)

Dimer **3b$_1$**. Synthesis (1:1 mM, PcL or MtL) and isolation as described above. R_f (HPLC) 4.3 min, UV–Vis (MeOH) λ_{max} 215, 269, 457 nm.

Dimer **3b$_2$** Synthesis (1:1 mM, PcL or MtL) and isolation as described above. R_f (HPLC) 4.9 min, UV–Vis (MeOH) λ_{max} 217, 265, 469 nm.

Dimer **3c**. Synthesis (1:1 mM, PcL or MtL) and isolation as described above. R_f (HPLC) 7.2 min, UV–Vis (MeOH) λ_{max} 217, 265, 469 nm. HRMS FT-ICR ($C_{16}H_{20}N_2O_7$) calcd: [M] 352.12704; found: $[M + Na]^+$ *m/z* 375.11824 (5.28 ppm).

Dimer **3d**. Synthesis (1:1 mM, PcL or MtL) and isolation as described above. R_f (HPLC) 8.3 min, UV–Vis (MeOH) λ_{max} 218, 272, 482 nm. HRMS FT-ICR ($C_{17}H_{23}N_3O_7$) calcd: [M] 381.15359; found: $[M + H]^+$ *m/z* 382.16244 (4.15 ppm), $[M + Na]^+$ *m/z* 404.14447 (4.11 ppm)

Dimer **3e**. Synthesis (1:1 mM, PcL or MtL) and isolation as described above. R_f (HPLC) 7.0 min, UV–Vis (MeOH) λ_{max} 215, 269, 457 nm. HRMS FT-ICR ($C_{16}H_{20}N_2O_7$) calcd: [M] 352.12704; found: $[M + H]^+$ *m/z* 353.13625 (5.51 ppm), $[M + Na]^+$ *m/z* 375.11832 (5.49 ppm).

Dimer **3f**. Synthesis (1:1 mM, PcL or MtL) and isolation as described above. R_f (HPLC) 7.8 min, UV–Vis (MeOH) λ_{max} 213, 271, 479 nm. HRMS FT-ICR ($C_{17}H_{23}N_3O_7$) calcd: [M] 381.15359; found: $[M + H]^+$ *m/z* 382.16254 (4.41 ppm), $[M + Na]^+$ *m/z* 404.14487 (5.10 ppm)

Dimer **3g$_1$**. Synthesis (1:1 mM, PcL or MtL) and isolation as described above. R_f (HPLC) 7.1 min, UV–Vis (MeOH) λ_{max} 212, 271, 479 nm.

Dimer **3g$_2$**. Synthesis (1:1 mM, PcL or MtL) and isolation as described above. R_f (HPLC) 7.5 min, UV–Vis (MeOH) λ_{max} 212, 273, 489 nm.

MS (of the product mixture **3g$_1$** and **3g$_2$**): *m/z*: AP-ES, pos. ion mode 503 $[M + H]^+$, 525 $[M + Na]^+$; ($C_{24}H_{30}N_4O_8$) calcd: [M] 502.

Dimer **3h**. Synthesis (1:2 mM and MtL) and isolation as described above. R_f (HPLC) 5.8 min, UV–Vis (MeOH) λ_{max} 219, 293, 488 nm. AP-ES ($C_{24}H_{29}N_3O_8$) calcd: [M] 487.195465; found: pos. ion mode $[M + H]^+$ *m/z* 488.201872 (1.78 ppm); neg. ion mode $[M - H]^-$ *m/z* 486.190211 (6.42 ppm) molecular mass for the quinoid product. ^{1}H NMR (D_2O) δ 1.01 (m, $J = 7.5$, 7.9 Hz, H4″), 1.49 (m, $J = 7.5$, 7.3 Hz, H5″), 1.55 (m, $J = 7.8$ Hz, H3″), 2.33 (t, $J = 7.7$ Hz, H8), 2.67 (m, $J = 7.5$ Hz, H7b), 2.63 (m, $J = 7.5$ Hz, H7a), 2.94 (t, $J = 7.4$ Hz, H6″), 3.07 (m, H7′), 4.10 (m, $J = 7.8$ Hz, H2″), 4.13 (m, H8′), 6.34 (s, H3), 6.69 (s, H6), 6.86 (d, $J = 7.5$ Hz, H3′, H5′), 7.20 (d, $J = 7.6$ Hz, H2′, H6′). ^{13}C-NMR (D_2O) δ 24.7 (C4″), 29.3 (C5″), 29.4 (C7), 34.4 (C3″), 40.3 (C7′), 40.4 (C8), 42.3 (C6″), 57.4 (C2″), 64.4 (C8′), 107.0 (C3), 118.7 (C3′/C5′), 120.6 (C6), 124.1 (C1), 131.7 (C1′), 133.6 (C2′/C6′), 139.8 (C5), 140.5 (C2), 145.7 (C4), 157.4 (C4′), 185.0 (C9). HMBC ^{1}H-^{13}C correlations H3 (C1, C4, C5), H6 (C2, C4, C7), H7a (C1, C2, C8), H7b (C1, C6, C8), H8 (C1, C7, C9), H2′/H6′ (C2′, C4′, C6′, C7′), H3′/H5′ (C1′, C3′, C5′), H8′ (C7′), H2″ (C3″), H3″ (C2″, C4″), H4″ (C3″, C5″), H5″ (C4″, C6″), H6″ (C4″, C5″) NMR data for the hydroquinoid product.

Dimer **3i**. Synthesis (1:1 mM, PcL or MtL) and isolation as described above. R_f (HPLC) 10.6 min, UV–Vis (MeOH) λ_{max} 212, 273, 480 nm. MS: *m/z*: AP-ES, pos. ion mode 637 $[M + H]^+$, 659 $[M + Na]^+$; ($C_{32}H_{36}N_4O_{10}$) calcd: [M] 636. AP-ES ($C_{32}H_{36}N_4O_{10}$) calcd: [M] 636.243144; found: pos. ion mode $[M + H]^+$ *m/z* 637.258109 (12.07 ppm); neg. ion mode $[M - H]^-$ *m/z* 635.240286 (8.68 ppm)

Trimer **4a**. Synthesis (1:10 mM, PcL) and isolation as described above. R_f (HPLC) 8.0 min, UV–Vis (MeOH) λ_{max} 285, 321, 499 nm. MS (LC/MS): *m/z*: AP-ES, pos. ion mode 525 $[M + H]^+$, 547 $[M + Na]^+$; HRMS FT-ICR ($C_{26}H_{24}N_2O_{10}$) calcd: [M] 524.14309; found: $[M + H]^+$ *m/z* 525.15109 (1.39 ppm), $[M + Na]^+$ *m/z* 547.13295 (1.17 ppm)

Trimer **4b$_1$**. Synthesis (1:10 mM, MtL) and isolation as described above. R_f (HPLC) 6.2 min, UV–Vis (MeOH) λ_{max} 212, 252(s), 345, 503 nm. MS and NMR data are the same as those of **4b$_2$** except from the following NMR data of the quinone moiety: ^{1}H NMR (D_2O) δ 5.22 (s, 2H). ^{13}C-NMR (D_2O) δ 95.2. HMBC ^{1}H-^{13}C correlations H 5.22 (C 156.3, C 180.4).

Trimer **4b$_2$**. Synthesis (1:10 mM, MtL) and isolation as described above. R_f (HPLC) 7.1 min, UV–Vis (MeOH) λ_{max} 212, 252(s), 345, 503 nm. AP-ES ($C_{22}H_{32}N_4O_8$) calcd: [M] 480.222014; found: pos. ion mode $[M + H]^+$ *m/z* 481.233060 (7.84 ppm), $[M + Na]^+$ *m/z* 503.214047 (5.59 ppm). ^{1}H NMR (D_2O) δ 1.39 (m, 4H, H4/H3″), 1.67 (m, 4H, H5/H2″), 1.70 (m, 2H, H3/H4″), 1.82 (m, 2H, H3/H4″), 2.02 (s, 6H, H8/H8″), 3.28 (m, 4H, H6/H1″), 4.14 (dd, 2H, H2/H5″), 5.36 (s, 2H, H2′/H5′). ^{13}C-NMR (D_2O) δ 24.7 (C8/C8″), 25.5 (C4/C3″), 29.8 (C5/C2″), 34.0 (C3/C4″), 45.1 (C6/C1″), 57.9 (C2/C5″), 94.8 (C2′/C5′), 156.8 (C1′/C4′), 176.5 (C7/C7″), 180.1 (C3′/C6′), 182.2 (C1/C6″). HMBC ^{1}H-^{13}C correlations H2/H5″ (C1/C6″, C3/C4″, C4/C3″, C7/C7″), H3/H4″ (C1/C6″, C2/C5″, C4/C3″, C5/C2″), H4/H3″ (C2/C5″, C5/C2″, C6/C1″), H5/H2″ (C3/C4″, C4/C3″, C6/C1″), H6/H1″ (C4/C3″, C5/C2″, C1′/C4′), H8/H8″ (C2/C5″, C7/C7″), H2′/H5′ (C4′/C1′, C6′/C3′).

Trimer **4b$_3$**. Synthesis (1:10 mM, MtL) and isolation as described above. HPLC/UV–Vis, MS, and NMR data are

the same as those of **4b$_2$** except from the following NMR data of the quinone moiety: ^{1}H NMR (D_2O) δ 5.39 (s, 2H). ^{13}C-NMR (D_2O) δ 94.8. HMBC ^{1}H-^{13}C correlations H 5.39 (C 156.5, C 181.3).

Trimer **4c**. Synthesis (1:10 mM, PcL) and isolation as described above. R_f (HPLC) 7.9 min, UV–Vis (MeOH) λ_{max} 212, 278, 349, 503 nm. AP-ES ($C_{25}H_{37}N_5O_{10}$) calcd: [M] 567.254043; found: pos. ion mode $[M + H]^+$ *m/z* 568.262128 (1.43 ppm), $[M + Na]^+$ *m/z* 590.243015 (0.42 ppm). ^{1}H NMR (D_2O) δ 1.38 (m, 2H, H4), 1.42 (m, 2H, H3″), 1.67 (m, 2H, H2″), 1.67 (m, 2H, H5), 1.70 (m, 1H, H3), 1.70 (m, 1H, H4″), 1.82 (m, 1H, H3), 1.82 (m, 1H, H4″), 2.01 (s, 3H, H8), 2.02 (s, 3H, H8″), 3.30 (t, $J = 6.3$ Hz, 2H, H1″), 3.37 (t, $J = 6.6$ Hz, 2H, H6), 3.46 (t, $J = 5.5$ Hz, 2H, H9′), 3.75 (t, $J = 5.5$ Hz, 2H, H10′), 4.18 (dd, 1H, H2, H5″), 5.48 (s, 1H, H5′). ^{13}C-NMR (D_2O) δ 24.6 (C8), 24.6 (C8″), 25.2 (C4), 25.2 (C3″), 29.6 (C2″), 31.1 (C5), 33.6 (C3), 33.6 (C4″), 45.1 (C1″), 46.5 (C6), 44.9 (C9′), 57.3 (C2), 57.3 (C5″), 62.6 (C10′), 94.8 (C5′), 106.7 (2′), 152.2 (C1′), 155.5 (C4′), 176.3 (C7/C7″), 177.9 (C3′), 180.2 (C6′), 180.9 (C1/C6″). HMBC ^{1}H-^{13}C correlations H1″ (C2″, C3″, C4′), H2 (C1, C3, C4, C7), H2″ (C3″), H3 (C1, C2, C4, C5), H3″ (C2″, C4″, C5″), H4 (C2, C3, C5, C6), H4″ (C2″, C3″, C5″, C6″), H5 (C4), H5″ (C3″, C4″, C6″, C7″), H6 (C1′, C4, C5), H8 (C2, C7), H8″ (C5″, C7″), H9′ (C7′, C10′), H10′ (C9′).

Trimer **4d$_1$**. Synthesis (1:1 mM, PcL or MtL) and isolation as described above. R_f (HPLC) 6.5 min, UV–Vis (MeOH) λ_{max} 212, 275, 349 nm

Trimer **4d$_2$**. Synthesis (1:1 mM, PcL or MtL) and isolation as described above. R_f (HPLC) 7.4 min, UV–Vis (MeOH) λ_{max} 212, 275, 350 nm

Trimer **4d$_3$**. Synthesis (1:1 mM, PcL or MtL) and isolation as described above. R_f (HPLC) 8.7 min, UV–Vis (MeOH) λ_{max} 212, 275, 349 nm

Trimer **4d$_4$**. Synthesis (1:1 mM, PcL or MtL) and isolation as described above. R_f (HPLC) 9.4 min, UV–Vis (MeOH) λ_{max} 212, 275, 347 nm

MS (of the product mixture **4d$_1$**–**4d$_4$**): *m/z* AP-ES, pos. ion mode 810 $[M + H]^+$, 832 $[M + Na]^+$; ($C_{24}H_{30}N_4O_8$) calcd: [M] 809.

Trimer **4e$_1$**. Synthesis (1:10 mM, PcL) and isolation as described above. R_f (HPLC) 7.1 min, UV–Vis (MeOH) λ_{max} 224, 275, 399 nm

Trimer **4e$_2$**. Synthesis (1:10 mM, PcL) and isolation as described above. R_f (HPLC) 8.4 min, UV–Vis (MeOH) λ_{max} 224, 272, 395 nm. AP-ES ($C_{39}H_{48}N_6O_{11}$) calcd: $[M - H_2O]$ 776.338107; found: pos. ion mode $[M - H_2O + H]^+$ *m/z* 777.344541 (1.08 ppm); neg. ion mode $[M - H_2O - H]^-$ *m/z* 775.330408 (0.87 ppm)

Trimer **4e$_3$**. Synthesis (1:10 mM, PcL) and isolation as described above. R_f (HPLC) 8.4 min, UV–Vis (MeOH) λ_{max} 224, 272, 395 nm. AP-ES ($C_{39}H_{48}N_6O_{11}$) calcd: $[M - H_2O]$ 776.338107; found: pos. ion mode $[M - H_2O + H]^+$ *m/z* 777.343541 (2.35 ppm); neg. ion mode $[M - H_2O - H]^-$ *m/z* 775.330158 (0.55 ppm)

ESI–MS/MS measurement of a trimer mixture **4e** resulted in 3 different products: calcd: $[M - H_2O]$ 776.338107; found: pos. ion mode $[M - H_2O + H]^+$ *m/z* 389.1767, 389.1768, and 389.1770 (z = 2).

^{1}H NMR (D_2O) of four trimers from a product mixture **first trimer** δ 1.30–1.83 (4×m, 6×CH_2), 2.39 (t, $J = 7.1$ Hz, 2H, CH_2), 2.94 (t, $J = 7.6$ Hz, 2H, CH_2), 3.21–3.92 (6×m, 4×CH_2, 2×CH), 4.20 (dd, 2H, 2×CH), 6.33 (s, 1H, CH), 6.85 (d, $J = 8.5$ Hz, 4H, 4×CH), 7.18 (d, $J = 8.3$ Hz, 4H, 4×CH); **second trimer** δ 1.30–1.83 (4×m, 6×CH_2), 2.39 (t, $J = 7.1$ Hz, 2H, CH_2), 2.94 (t, $J = 7.6$ Hz, 2H, CH_2), 3.21–3.92 (6×m, 4×CH_2, 2×CH), 4.20 (dd, 2H, 2×CH), 5.55 (s, 1H, CH), 6.85 (d, $J = 8.5$ Hz, 4H, 4×CH), 7.18 (d, $J = 8.3$ Hz, 4H, 4×CH); **third trimer** δ 1.40–1.69 (4×m, 6×CH_2), 2.34 (t, $J = 7.6$ Hz, 2H, CH_2), 2.85 (2×t, $J = 7.5$ Hz, 2H, CH_2), 3.04–3.95 (4×m, 4×CH_2, 2×CH), 4.11 (dd, 2H, 2×CH), 6.71 (s, 1H, CH), 6.88 (d, $J = 7.7$ Hz, 4H, 4×CH), 7.20 (d, $J = 7.4$ Hz, 4H, 4×CH); **fourth trimer** δ 1.40–1.69 (4×m, 6×CH_2), 2.34 (t, $J = 7.6$ Hz, 2H, CH_2), 2.85 (2×t, $J = 7.5$ Hz, 2H, CH_2), 3.04–3.95 (4×m, 4×CH_2, 2×CH), 4.11 (dd, 2H, CH), 5.28 (s, 1H, CH), 6.88 (d, $J = 7.7$ Hz, 4H, 4×CH), 7.20 (d, $J = 7.4$ Hz, 4H, 4× CH).

Trimer **4f$_1$**. Synthesis (1:10 mM, PcL) and isolation as described above. R_f (HPLC) 10.2 min, UV–Vis (MeOH) λ_{max} 212, 273, 345 nm

Trimer **4f$_2$**. Synthesis (1:10 mM, PcL) and isolation as described above. R_f (HPLC) 11.7 min, UV–Vis (MeOH) λ_{max} 212, 277, 347 nm

MS (of the product mixture **4f$_1$** and **4f$_2$**): *m/z*: AP-ES, pos. ion mode 1,078 $[M + H]^+$, 1,100 $[M + Na]^+$; ($C_{32}H_{36}N_4O_{10}$) calcd: [M] 1,077. AP-ES ($C_{32}H_{36}N_4O_{10}$) calcd: [M] 1,077.433129; found: pos. ion mode $[M + H]^+$ *m/z* 1,078.443139 (2.54 ppm); neg. ion mode $[M - H]^-$ *m/z* 1,076.429393 (4.31 ppm).

After digestion of the polymer mixture **5a** using Lys C, three products were detected by ESI–MS/MS, which correspond to products **4e**. calcd: $[M - H_2O]$ 776.338107; found: pos. ion mode $[M - H_2O + H]^+$ *m/z* 389.1768, 389.1771, and 389.1770, (z = 2), fragmentation: 129.08, 147.06, 293.27, 302.29, 380.24, 457.16, 485.28, 585.27, 603.27, 631.28, 649.22.

Results and discussion

The laccase-catalyzed reactions of four amino acids **1a–1d** and two dipeptides **1e** and **1f** with dihydroxylated aromatics **2a–2d** were analyzed by HPLC using a diode array

detector. Diverse product patterns of dimers and trimers were detected (Table 1). Some of the dimers (termed **3**) and some of the trimers (termed **4**) were detected in higher concentration and were sufficiently stable for isolation and further structural characterization.

Reaction of tyrosine, lysine, and lysine derivatives with dihydroxylated aromatic compounds

L-Tyrosine **1a** and L-lysine **1b** were subjected to laccase-catalyzed transformation of 2,5-dihydroxybenzoic acid methyl ester **2a**. L-Lysine was used as it, besides DOPA, is another major component of synthetic DOPA-containing polypeptides and because it (1) is present in large quantities in MAPs, (2) is thought to be involved in protein cross-linking reactions (Holl et al. 1993), and (3) provided good water solubility to copolymers (Deming 2007).

L-Tyrosine was used as it is a precursor of DOPA (Marumo and Waite 1986), less reactive than DOPA and because it is also a component of MAPs (Waite et al. 1985; Rzepecki et al. 1991).

The laccase-catalyzed reactions of L-tyrosine **1a** with 2,5-dihydroxybenzoic acid methyl ester **2a** resulted in one C–N coupling dimer **3a** (equimolar reaction mixture) and one C–N coupling trimer **4a** (1:10 mM reaction mixture) both of which were readily detected by HPLC using a diode array detector (Table 1). **3a** consists of one *p*-quinone and one amino acid moiety, whereas **4a** consists of the *p*-quinone component plus two amino acid molecules as described for other amination products (Niedermeyer et al. 2005; Hahn et al. 2009a). The identification of the cross-couplings between **2a** and L-tyrosine is based on UV–Vis and mass spectral data listed in "Materials and methods".

Whereas L-tyrosine has only the α-amino group with which to aminate the laccase substrate and hence can produce only one dimer and one trimer, L-lysine has both the α- and the ε-amino group. Since the acid–base ionization/dissociation constants (p*K*a) of the α-amino group (9.2) is lower than that of the ε-amino group (10.3) the α-amino group should react better than the ε-amino group. Nevertheless, if both the α- and the ε-amino group are able to react with the *para*-dihydroxylated compounds L-lysine can aminate twice to produce different dimers, trimers, and oligomers. As shown by the cross-linked products of α-amino acids (Hahn et al. 2009a) and other primary amines (Niedermeyer et al. 2005; Mikolasch et al. 2007) the preferred binding position of the first amino group is the *ortho*-position of the carbonyl group of the *para*-dihydroxylated aromatics. The second amine attacks at the *para*-position of the first amino group. Derived from these known binding positions, we postulated four possible trimer structures shown in Fig. 1 and a number of different oligomers consisting of various numbers of L-lysine and *para*-dihydroxylated laccase substrate. The laccase-catalyzed reaction of equimolar amounts of 2,5-dihydroxybenzoic acid methyl ester **2a** and L-lysine **1b** resulted in the formation of two dimers $\mathbf{3b_1}$ and $\mathbf{3b_2}$ with slightly different chromatographic behaviors (Table 1). The isolation and further structural characterization of the dimers did not lead to usable results because of their high reactivity and tendency to form higher molecular weight products. Therefore, we used the N-derivatized L-lysines Nα-acetyllysine **1c** (Ac-Lys-OH) and Nε-acetyllysine **1d** (Lys(Ac)-OH) for the laccase-catalyzed reaction with **2a.** In these reactions, we expect at most one dimer per reaction since both of the derivatized amino acids have only one free amino group for cross-linking. Indeed, **1c** and **1d** reacted rapidly to yield only one dimer (**3c** from **1c** and **3e** from **1d**) consisting of one *p*-quinone and one amino acid moiety, based on UV–Vis and mass spectral data listed in "Materials and methods".

As the UV–Vis spectra of $\mathbf{3b_1}$ (formed from **2a** and lysine) and **3e** (formed from **2a** and Lys(Ac)-OH) are identical (Table 1) we deduced that the free α-amino group of both **1b** and **1d** is responsible for the cross-link between **2a** and the amino acids. The UV–Vis spectra of $\mathbf{3b_2}$ (formed from **2a** and lysine) and **3c** (formed from **2a** and Ac-Lys-OH) are also equivalent (Table 1) and so the free ε-amino group of both **1b** and **1c** reacted with the laccase substrate **2a** to form dimers. This demonstrates that both amino groups of L-lysine are able to react with the laccase substrate **2a**. To further determine the bonding points between the amino acids and **2a** we tried to analyze the dimers with NMR. However, these attempts were vitiated by the low stability of highly concentrated solutions of the dimers in methanol and by their inadequate solubility in chloroform and water. These restrictions also applied to other dimers formed from *para*-hydroquinone **2b** or 2,5-dihydroxy-*N*-(2-hydroxyethyl)-benzamide **2c** with **1c** (Ac-Lys-OH) or **1d** (Lys(Ac)-OH) which could not be analyzed by MS or NMR. Since the design of potential biomaterial for biomedical or industrial applications requires the determination of the structure of the reaction products by MS and NMR, we synthesized trimers consisting of one molecule dihydroxylated aromatic compound and two molecules of amino acid. From the laccase-catalyzed reaction of *para*-hydroquinone **2b** (1 mM) and **1c** (Ac-Lys-OH; 10 mM) we obtained two trimers $\mathbf{4b_1}$ and $\mathbf{4b_2}$ with slightly different chromatographic behaviors (Table 1) and reasonable stability. Because of their similar retention times, the trimers could not be separated from each other by chromatography. MS and NMR analyses of the trimer mixture documented for $\mathbf{4b_2}$ (main product) the coupling of the ε-amino group of one molecule **1c** to the C1′-atom of $\mathbf{4b_2}$ and the coupling of the ε-amino group of a second

Table 1 Products obtained in laccase-catalyzed transformation

Reactants	2,5-Dihydroxy-benzoic acid methyl ester **2a**	*para*-Hydroquinone **2b**	2,5-Dihydroxy-*N*-(2-hydroxyethyl)-benzamide **2c**	Hydrocaffeic acid **2d**
L-Tyrosine **1a**	Dimer **3a**[a] (8.8)[b] (218, 273, 481)[c]	Dimer (7.8) (216, 266, 480)	Dimer (8,4) (221, 271, 481)	/[d]
	Trimer **4a** (8.0) (285, 321, 499)	Trimer (7.6) (210, 340, 480)	Trimer (8.0) (217, 273, 347)	
		Trimer (8.6) (212, 341, 492)	Trimer (8.9) (219, 275, 348)	
		Trimer (9.2) (210, 272, 342, 454)	Trimer (9.6) (219, 275, 349)	
L-Lysine **1b**	Dimer **3b$_1$** (4.3) (215, 269, 457)	Dimer (3.4) (214, 262, 482)	Dimer (4.9) (219, 271, 479)	/
	Dimer **3b$_2$** (4.9) (217, 265, 469)		Dimer (5.7) (219, 275, 481)	
	Some heteromolecular trimers and oligomers with overlapping chromatographic behavior	Trimer (3.7) (212, 344, 484)	Trimer (4.7) (215, 275, 349)	
			Trimer (5.3) (215, 275, 349)	
			Trimer (5.8) (215, 275, 347)	
			Trimer (6.5) (217, 273, 345)	
Ac-Lys-OH **1c**	Dimer **3c** (7.2) (217, 265, 469)	Dimer (6.2) (218, 262, 496)	Dimer **3d** (8.3) (218, 272, 482)	/
	–[e]	Trimer **4b$_1$** (6.2) (212, 252(s), 345, 503)	Trimer **4c** (7.9) (212, 278, 349, 503)	
		Trimer **4b$_2$** (7.1) (212, 252(s), 345, 503)		
		Trimer **4b$_3$** (7.1) (212, 252(s), 345, 503)		
Lys(Ac)-OH **1d**	Dimer **3e** (7.0) (215, 269, 457)	Dimer (6.2) (214, 261, 478)	Dimer **3f** (7.8) (213, 271, 479)	/
	Trimer (7.7) (273, 339)	Trimer (7.1) (342, 504)	Trimer (8.3) (211, 273, 488)	
		Trimer (6.2) (342)		
H-Tyr-Lys-OH **1e**	Some heteromolecular dimers and trimers with overlapping chromatographic behavior	Some heteromolecular dimers and trimers with overlapping chromatographic behavior	Dimer **3g$_1$** (7.1) (212, 271 479)	Dimer **3h** (5.8) (219, 293, 488)
			Dimer **3g$_2$** (7.5) (212, 273 489)	
			Trimer **4d$_1$** (6.5) (212, 275, 349)	Trimer **4e$_1$** (7.1) (224, 275, 399)
			Trimer **4d$_2$** (7.4) (212, 275, 350)	Trimer **4e$_2$** (8.4) (224, 272, 395)
			Trimer **4d$_3$** (8.7) (212, 275, 349)	Trimer **4e$_3$** and **4e$_4$** differ only in MS and NMR
			Trimer **4d$_4$** (9.4) (212, 275, 347)	
Z-[Tyr-Lys]-OH **1f**	/	/	Dimer **3i** (10.6) (212, 273, 480)	Dimer (9.5) (211, 283, 501)
			Trimer **4f$_1$** (10.2) (212, 273, 345)	–
			Trimer **4f$_2$** (11.7) (212, 277, 347)	
[Tyr-Lys]$_{10}$	/	/	Three-dimensional network	Three-dimensional network **5a**

[a] Product description only for MS and/or NMR analyzed products

[b] R_f-HPLC (in min) values in parentheses

[c] UV–Vis (MeOH) λ_{max} (in nm) values in parentheses

[d] Reaction not performed

[e] No products identified

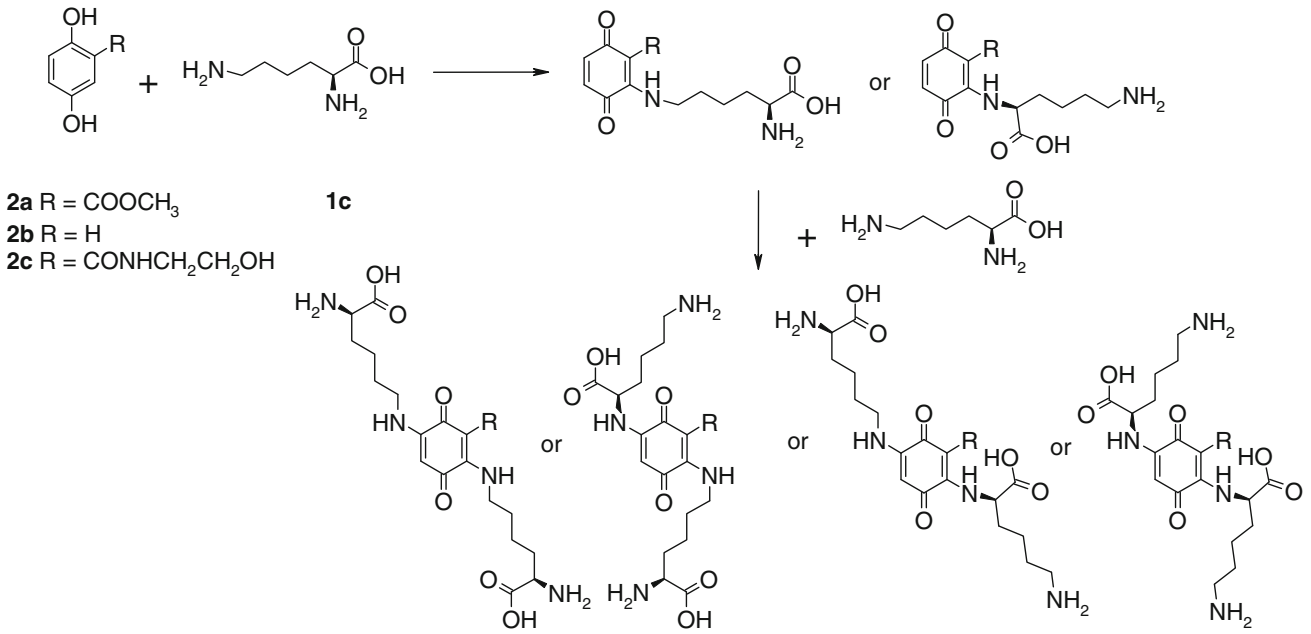

Fig. 1 Reactions of the α- and ε-amino group of lysine with dihydroxylated aromatic compounds forming dimers and trimers

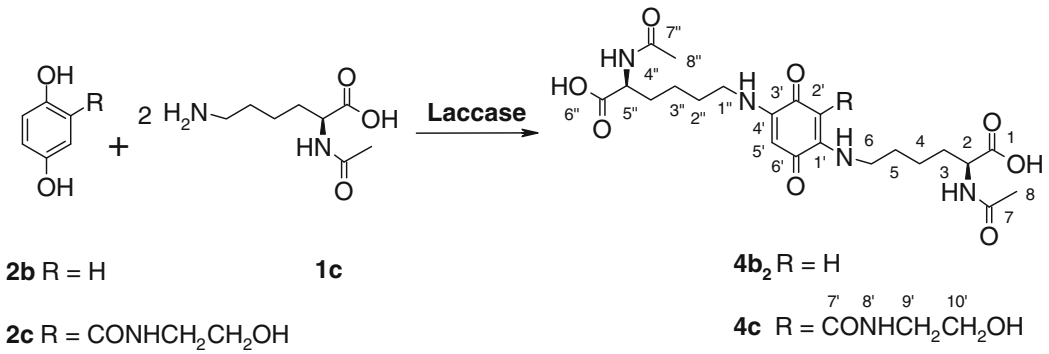

Fig. 2 *para*-Hydroquinone and 2,5-dihydroxy-*N*-(2-hydroxyethyl)-benzamide (laccase substrates **2b** and **2c**), Ac-Lys-OH (reactant **1c**), and the trimers $\mathbf{4b_2}$ and **4c** as products of laccase-catalyzed reactions

molecule **1c** to the C4′-atom of $\mathbf{4b_2}$ (Fig. 2). Therefore, the aminations occur in *para*-position to each other as previously described for structurally related trimers (Niedermeyer et al. 2005; Hahn et al. 2009a). In addition to the main trimer $\mathbf{4b_2}$ NMR analyses showed additional signals for two additional trimers in very small quantities, one of them may correspond to $\mathbf{4b_1}$ and the other to $\mathbf{4b_3}$, which probably has the same retention time as $\mathbf{4b_2}$. Due to the low-signal intensity, we could not determine the cross-linking points of $\mathbf{4b_1}$ and $\mathbf{4b_3}$. One trimer **4c** could be analyzed from the reaction of 2,5-dihydroxy-*N*-(2-hydroxyethyl)benzamide **2c** (1 mM) and **1c** (Ac-Lys-OH; 10 mM) which has a comparable structure to $\mathbf{4b_2}$ (Fig. 2). With the structures of $\mathbf{4b_2}$ and **4c**, we show that the ε-amino group of **1c** is able to cross-link dihydroxylated aromatics in different ways. This type of cross-linking of the ε-amino group has also been described by Wang et al. (1996) for a peptidyl lysine with the modified side chain of a tyrosyl residue. The cross-linked product was a lysine tyrosylquinone. Studies on adhesion mechanisms of MAPs have described adhesions, oxidations, and cross-linking reaction pathways for peptidyl DOPA and DOPA *ortho*-quinone; (i) formation of DOPA-metal complexes (Hansen and Waite 1991; Deming 1999; Ooka and Garrell 2000; Holten-Andersen et al. 2009a), (ii) adsorption of DOPA to metal- or metal-oxide-bearing surfaces through hydrogen bonding (McBride and Wesselink 1988; Deming, 1999), (iii) physical interactions rather than chemical bonding (Lin et al. 2007), (iv) reaction of DOPA or DOPA-quinone to form free radicals which result in dimeric cross-linked biarylic products (Waite 1990b, 1992; McDowell et al. 1999; Burzio et al. 2000), and (v) coupling of DOPA-

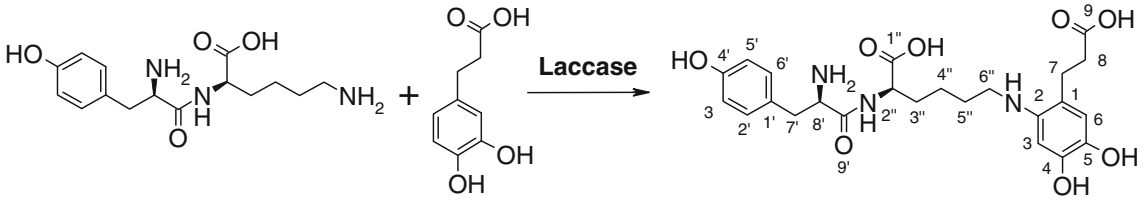

Fig. 3 H-Tyr-Lys-OH (reactant **1e**), hydrocaffeic acid (laccase substrates **2d**), and the dimer **3h** as a product of laccase-catalyzed reaction

quinone with a free amino group to form an inter chain imine cross-link or in a Michael addition reaction to form an amine cross-link (Waite 1990b; Yamamoto et al. 1997, 2000). Our results support thesis (v) the formation of amine cross-links. We have demonstrated that the ε-amino group of lysine is able to cross-link dihydroxylated aromatics.

Based on the results of the tyrosine and lysine cross-linking with dihydroxylated aromatics the laccase-catalyzed reaction of dipeptides consisting of tyrosine and lysine or their derivatives with dihydroxylated aromatics was the next step on the way to the development of potent biomaterial for biomedical or industrial applications.

Reactions of dipeptides and their derivatives with dihydroxylated aromatic compounds

The dipeptide H-Tyr-Lys-OH **1e** was subjected to laccase-catalyzed transformations with the dihydroxylated aromatic compounds: 2,5-dihydroxybenzoic acid methyl ester **2a**, *para*-hydroquinone **2b**, 2,5-dihydroxy-*N*-(2-hydroxyethyl)-benzamide **2c**, and hydrocaffeic acid **2d**. The reactions of 2,5-dihydroxy-*N*-(2-hydroxyethyl)-benzamide **2c** and of hydrocaffeic acid **2d** yielded products suitable for structural characterization.

The MS analysis of the reaction products of **1e** with 2,5-dihydroxy-*N*-(2-hydroxyethyl)-benzamide **2c** gave the dimer structures $\mathbf{3g_1}$ and $\mathbf{3g_2}$ as a mixture which consist of a quinone and a dipeptide moiety. In addition, the trimer products ($\mathbf{4d_1}$ to $\mathbf{4d_4}$ as a mixture) were shown to consist of one quinone and two dipeptide moieties. Due to the high reactivity of the dimers and trimers no satisfactory NMR analyses could be performed.

A hydroquinoid dimer **3h** (Fig. 3) was produced in the reaction of H-Tyr-Lys-OH **1e** (2 mM) and hydrocaffeic acid **2d** (1 mM) and this product was characterized by NMR, while a quinoid dimer analogous to those described for the other reactions was characterized by MS analysis. Together the NMR and the MS data support the notion of cross-linking between H-Tyr-Lys-OH and hydrocaffeic acid. Additional to the dimer product **3h** two trimers could be analyzed by MS and four trimers $\mathbf{4e_1}$, $\mathbf{4e_2}$, $\mathbf{4e_3}$, and $\mathbf{4e_4}$ were detected by NMR from a product mixture. However, due to the low signal intensity, we could only determine the existence of these four different trimers, but we could not assign the direct coupling points between H-Tyr-Lys-OH **1e** and hydrocaffeic acid **2d**. The structures may be similarly complex to the situation demonstrated for the reaction of lysine in Fig. 1 with both the free α-amino group of the Tyr-moiety and the free ε-amino group of the Lys moiety of **1e** being involved in the cross linking reactions.

We further tried to analyze the reactions of 2,5-dihydroxy-*N*-(2-hydroxyethyl)-benzamide **2c** and hydrocaffeic acid **2d** with Z-[Tyr-Lys]-OH **1f**. As expected, dimers and trimers were detected by HPLC. The MS analysis of the reaction products of **1f** with **2c** resulted in the description of one dimer **3i** consisting of a quinone and a dipeptide moiety and two further trimer products $\mathbf{4f_1}$ and $\mathbf{4f_2}$ each consisting of one quinone and two dipeptide moieties.

Our results with dipeptides support the thesis of the involvement of amine cross-links in the adhesion mechanisms of MAPs. The ε-amino group of lysine in dipeptides is able to cross-link dihydroxylated aromatics forming dimers and trimers and presumably higher molecular weight products. The next step on the way to potential biomaterials was to investigate the laccase-catalyzed reactions of dihydroxylated aromatics with oligopeptides.

Reactions of oligopeptides with dihydroxylated aromatic compounds

The oligopeptide with the structure $[\text{Tyr-Lys}]_{10}$ was used in laccase-catalyzed reactions with dihydroxylated aromatics since synthetic polypeptides have been previously used to mimic marine adhesives (Yu and Deming 1998; Yamamoto et al. 2000). The results obtained with L-lysine **1a** and the dipeptide H-Tyr-Lys-OH **1e** and the reported cross-linking of the ε-amino group of a peptidyl lysine with the modified side chain of a tyrosyl residue of a cofactor in lysyl oxidase (Wang et al. 1996) led us to expect three-dimensional networks to result from the reaction of $[\text{Tyr-Lys}]_{10}$ and 2,5-dihydroxy-*N*-(2-hydroxyethyl)-benzamide **2c** or hydrocaffeic acid **2d** (Fig. 4). These networks should be cross-linked by the free ε-amino groups of the Lys moiety of $[\text{Tyr-Lys}]_{10}$ and produce a variety of polymers. The reaction mixtures of $[\text{Tyr-Lys}]_{10}$ and 2,5-dihydroxy-*N*-(2-hydroxyethyl)-benzamide **2c** or hydrocaffeic acid **2d**

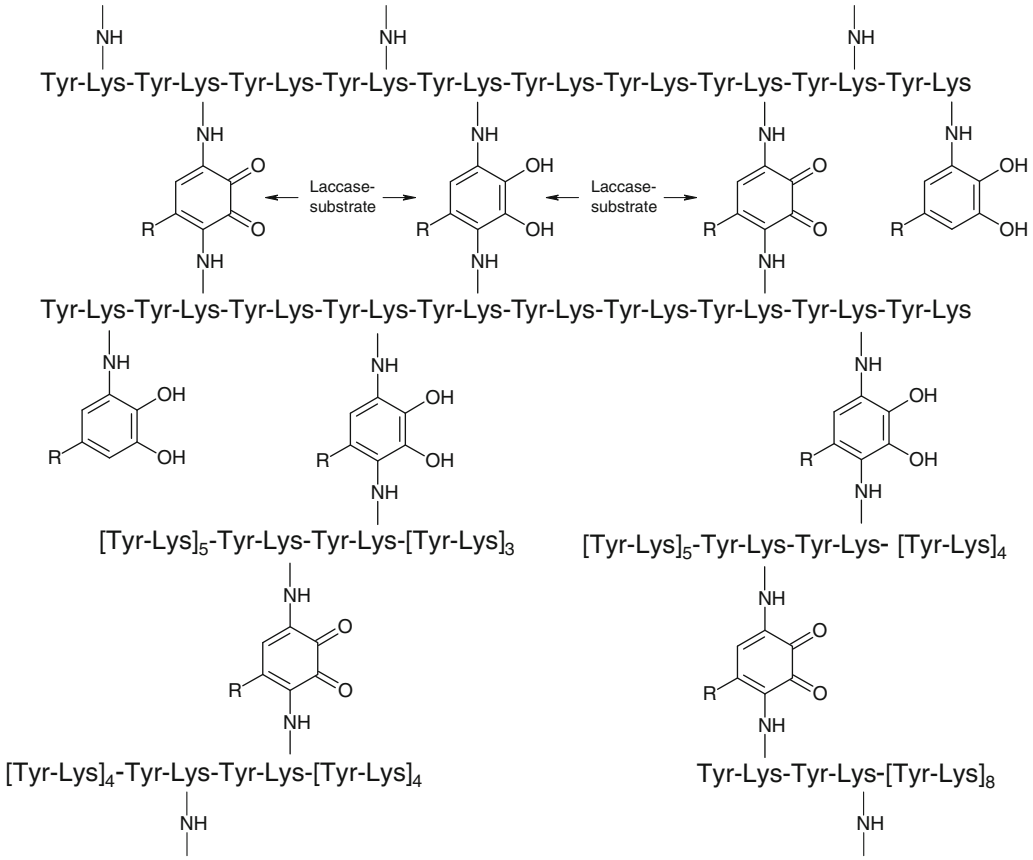

Fig. 4 Model of a three-dimensional network (**5a**) resulting from the laccase-catalyzed reaction of $[Tyr\text{-}Lys]_{10}$ and hydrocaffeic acid **2d** ($R=CH_2CH_2COOH$)

turned from colorless to brown with the formation of a brown precipitate and neither reaction products nor the reactants were detectable by HPLC. This suggests that high molecular weight products which are not isolable or analyzable by MS or NMR were formed in this reaction. $[Tyr\text{-}Lys]_{10}$ contains ten free ε-amino groups some or all of which may react with laccase substrate molecules to form diverse structures. To determine the cross-link between $[Tyr\text{-}Lys]_{10}$ and the dihydroxylated aromatics the polymer mixture **5a** of $[Tyr\text{-}Lys]_{10}$ and hydrocaffeic acid **2d** was digested with lys C, which cleaves the bonds between the Tyr-Lys-units of the oligopeptide forming low-molecular weight products including the trimers like **4e$_1$**–**4e$_4$**. The digested mixture was analyzed by MS and the MS data were compared with those of the trimer mixture formed from H-Tyr-Lys-OH **1e** and **2d**. In both analyses the mass of trimers **4e** (mixture of **4e$_1$**–**4e$_4$**) was detected indicating the cross-link of free ε-amino groups of $[Tyr\text{-}Lys]_{10}$ with hydrocaffeic acid **2d**. Hydrocaffeic acid is an *ortho*-dihydroxylated aromatic compound structurally related to DOPA. The single difference is the missing amino group of hydrocaffeic acid. Because of this, and taking into account the results described here, it appears that the adhesion mechanisms of MAPs derive, at least in part, from Michael addition reaction to form amine cross-link as suggested by (Waite 1990b; Burzio et al. 1997; Yamamoto et al. 1997, 2000).

Several potential medical applications have been proposed for MAPs because of their adhesive properties (Strausberg and Link 1990; Green 1995; Robin et al. 1988; Holten-Andersen and Waite 2008). In addition, they have been proposed as immobilizing agents for enzymes, cells, and tissues, as well as anti-corrosives, and metal scavenger agents (Deming 1999; Waite 2008).

Due to the three-dimensional network formation and the detected cross-link of free ε-amino groups of $[Tyr\text{-}Lys]_{10}$ our system of the three components—$[Tyr\text{-}Lys]_{10}$, dihydroxylated aromatic substrate and laccase—has potential as biomaterial for application in medicine or industry. The properties of our products have to be analyzed in further investigations for different applications.

Acknowledgments Financial support from the government of Mecklenburg-Vorpommern and from the European Union (Landesforschungsschwerpunkt „Neue Wirkstoffe und Biomaterialien – Innovative Screeningverfahren and Produktentwicklung'', Stiftung Industrieforschung „Weich- und Hartteilkleber für medizinische

Anwendungen, hergestellt durch Vernetzung von Proteinen durch Polyphenoloxidasen, in Kombination mit Blutstillung Projekt-Nr. S 752) and from Stryker Trauma GmbH (Schönkirchen), from Aesculap AG & Co. KG (Tuttlingen), and from BSN medical GmbH & Co.KG (Hamburg) is gratefully acknowledged. We thank R. Jack (Institute of Immunology, University of Greifswald) for help in preparing the manuscript.

References

Amster IJ (1996) Fourier transform mass spectrometry. J Mass Spectrom 31:1325–1337

Berka RM, Schneider P, Golightly EJ, Brown SH, Madden M, Brown KM, Halkier T, Mondorf K, Xu F (1997) Characterization of the gene encoding an extracellular laccase of *Myceliophthora thermophila* and analysis of the recombinant enzyme expressed in *Aspergillus oryzae*. Appl Environ Microbiol 63:3151–3157

Bourbonnais R, Paice MG (1990) Oxidation of nonphenolic substrates—an expanded role for laccase in lignin biodegradation. FEBS Lett 267:99–102

Braun-Lüllemann A, Majcherczyk A, Hüttermann A (1997) Degradation of styrene by white-rot fungi. Appl Microbiol Biotechnol 47:150–155

Burzio LO, Burzio VA, Silva T, Burzio LA, Pardo J (1997) Environmental bioadhesion: themes and applications. Curr Opin Biotechnol 8:309–312

Burzio LA, Burzio VA, Pardo J, Burzio LO (2000) In vitro polymerization of mussel polyphenolic proteins catalyzed by mushroom tyrosinase. Comp Biochem Physiol B Biochem Mol Biol 126:383–389

Deming TJ (1999) Mussel byssus and biomolecular materials. Curr Opin Chem Biol 3:100–105

Deming TJ (2007) Synthetic polypeptides for biomedical applications. Prog Polym Sci 32:858–875

Donat S, Streker K, Schirmeister T, Rakette S, Stehle T, Liebeke M, Lalk M, Ohlsen K (2009) Transcriptome and functional analysis of the eukaryotic-type serine/threonine kinase PknB in *Staphylococcus aureus*. J Bacteriol 191:4056–4069

Eggert C, Temp U, Eriksson KEL (1996) The ligninolytic system of the white rot fungus *Pycnoporus cinnabarinus*: purification and characterization of the laccase. Appl Environ Microbiol 62:1151–1158

Feng BB, Voehler M, Zhou L, Passarelli M, Harris CM, Harris TM, Stone MP (1996) Major groove (S)-α-(N6-Adenyl)styrene oxide adducts in an oligodeoxynucleotide containing the human N-ras codon 61 sequence: conformation of the S (61, 2) and S (61, 3) sequence isomers from 1H NMR. Biochemistry 35:7316–7329

Green K (1995) Mussel adhesive protein. In: Sierra DH, Saltz R (eds) Surgical adhesives and sealants. Current technology and applications. Technomic, Lancaster, pp 19–27

Hahn V, Mikolasch A, Manda K, Gördes D, Thurow K, Schauer F (2009a) Derivatization of amino acids by fungal laccases: comparison of enzymatic and chemical methods. J Mol Catal B Enzym 60:76–81

Hahn V, Mikolasch A, Manda K, Gördes D, Thurow K, Schauer F (2009b) Laccase-catalyzed carbon-nitrogen bond formation: coupling and derivatization of unprotected L-phenylalanine with different *para*-hydroquinones. Amino Acids 37:315–321

Hansen DC, Waite JH (1991) Marine metal chelating proteins. Am Chem Soc Symp Ser 444:256–262

Harrington MJ, Waite JH (2007) Holdfast heroics: comparing the molecular and mechanical properties of *Mytilus californianus* byssal threads. J Exp Biol 210:4307–4318

Holl SM, Hansen D, Waite JH, Schaefer J (1993) Solid-state NMR analysis of cross-linking in mussel protein glue. Arch Biochem Biophys 302:255–258

Holten-Andersen N, Waite JH (2008) Mussel-designed protective coatings for compliant substrates. J Dent Res 87:701–709

Holten-Andersen N, Mates TE, Toprak MS, Stucky GD, Zok FW, Waite JH (2009a) Metals and the integrity of a biological coating: the cuticle of mussel byssus. Langmuir 25:3323–3326

Holten-Andersen N, Zhao H, Waite JH (2009b) Stiff coatings on compliant biofibers: the cuticle of *Mytilus californianus* byssal threads. Biochemistry 48:2752–2759

Jonas U, Hammer E, Schauer F, Bollag JM (1998) Transformation of 2-hydroxydibenzofuran by laccases of the white rot fungi *Trametes versicolor* and *Pycnoporus cinnabarinus* and characterization of oligomerization products. Biodegradation 8:321–328

Lin Q, Gourdon D, Sun CJ, Holten-Andersen N, Anderson TH, Waite JH, Israelachvili JN (2007) Adhesion mechanisms of the mussel foot proteins mfp-1 and mfp-3. Proc Natl Acad Sci USA 104:3782–3786

Manda K, Hammer E, Mikolasch A, Gördes D, Thurow K, Schauer F (2006) Laccase-induced derivatization of unprotected amino acid L-tryptophan by coupling with *p*-hydroquinone 2,5-dihydroxy-*N*-(2-hydroxyethyl)-benzamide. Amino Acids 31:409–419

Marshall AG, Schweikhard L (1992) Fourier-transform ion-cyclotron resonanc mass-spectrometry—technique developments. Int J Mass Spectrom Ion Processes 118(119):37–70

Marshall AG, Hendrickson CL, Jackson GS (1998) Fourier transform ion cyclotron resonance mass spectrometry: a primer. Mass Spectrom Rev 17:1–35

Marumo K, Waite JH (1986) Optimization of hydroxylation of tyrosine and tyrosine-containing peptides by mushroom tyrosinase. Biochim Biophys Acta 872:98–103

McBride MB, Wesselink LG (1988) Chemisorption of catechol on gibbsite, boehmite, and noncrystalline alumina surfaces. Environ Sci Technol 22:703–708

McDowell LM, Burzio LA, Waite JH, Schaefer J (1999) Rotational echo double resonance detection of cross-links formed in mussel byssus under high-flow stress. J Biol Chem 274:20293–20295

Mikolasch A, Niedermeyer THJ, Lalk M, Witt S, Seefeldt S, Hammer E, Schauer F, Gesell M, Hessel S, Jülich WD, Lindequist U (2007) Novel cephalosporins synthesized by amination of 2,5-dihydroxybenzoic acid derivatives using fungal laccases. Chem Pharm Bull 55:412–416

Niedermeyer THJ, Mikolasch A, Lalk M (2005) Nuclear amination catalyzed by fungal laccases: reaction products of *p*-hydroquinones and primary aromatic amines. J Org Chem 70:2002–2008

Ooka AA, Garrell RL (2000) Surface-enhanced Raman spectroscopy of DOPA-containing peptides related to adhesive protein of marine mussel, *Mytilus edulis*. Biopolymers 57:92–102

Robin JB, Picciano P, Kusleika RS, Salazar J, Benedict C (1988) Preliminary evaluation of the use of mussel adhesive protein in experimental epikeratoplasty. Arch Ophthal 106:973–977

Rzepecki LM, Chin SS, Waite JH, Lavin MF (1991) Molecular diversity of marine glues: polyphenolic proteins from five mussel species. Mol Mar Biol Biotechnol 1:78–88

Strausberg RL, Link RP (1990) Protein-based medical adhesives. Trends Biotechnol 8:53–57

Vreeland V, Waite JH, Epstein L (1998) Polyphenols and oxidases in substratum adhesion by marine algae and mussels. J Phycol 34:1–8

Waite JH (1990a) Marine adhesive proteins—natural composite thermosets. Int J Biol Macromol 12:139–144

Waite JH (1990b) The phylogeny and chemical diversity of quinone-tanned glues and varnishes. Comp Biochem Physiol 97B:19–29

Waite JH (1992) The DOPA ephemera—a recurrent motif in invertebrates. Biol Bull 183:178–184

Waite JH (2008) Surface chemistry—Mussel power. Nat Mater 7:8–9

Waite JH, Housley TJ, Tanzer ML (1985) Peptide repeats in a mussel glue protein: theme and variations. Biochemistry 24:5010–5014

Waite JH, Hansen DC, Little KT (1989) The glue protein of ribbed mussels (*Geukensia demissa):* a natural adhesive with some features of collagen. J Comp Physiol B 159:517–525

Wang SX, Mure M, Medzihradszky KF, Burlingame AL, Brown DE, Dooley DM, Smith AJ, Kagan HM, Klinmant JP (1996) A crosslinked cofactor in lysyl oxidase: redox function for amino acid side chains. Science 273:1078–1084

Yamamoto H, Hayakawa T (1979) Synthesis of sequential polypeptides containing L-beta-3,4-dihydroxyphenyl-alpha-alanine (Dopa) and L-glutamic acid. Biopolymers 18:3067–3076

Yamamoto H, Hayakawa T (1982) Synthesis of sequential polypeptides containing L-beta-3,4-dihydroxyphenyl-alpha-alanine (Dopa) and L-lysine. Biopolymers 21:1137–1151

Yamamoto H, Ogawa T, Nishida A (1997) Studies on quinone cross-linking adhesion mechanism and preparation of antifouling surfaces toward the blue mussel. J Mar Biotechnol 5:133–136

Yamamoto H, Sakai Y, Ohkawa K (2000) Synthesis and wettability characteristics of model adhesive protein sequences inspired by a marine mussel. Biomacromolecules 1:543–551

Yu M, Deming TJ (1998) Synthetic polypeptide mimics of marine adhesive. Macromolecules 31:4739–4745

Zhao H, Waite JH (2006) Linking adhesive and structural proteins in the attachment plaque of *Mytilus californianus*. J Biol Chem 281:26150–26158

Zhao H, Robertson NB, Jewhurst SA, Waite JH (2006) Probing the adhesive footprints of *Mytilus californianus* byssus. J Biol Chem 281:11090–11096